Received: Added at production | Revised: Added at production | Accepted: Added at production

DOI: xxx/xxxx

RESEARCH ARTICLE

# Impacts of low stratocumulus clouds on offshore wind farm power

Pim van Dorp[1] | Anda Knol[2] | Stephan R. de Roode[2] | Harm J. J. Jonker[1,2] | Remco A. Verzijlbergh[1,3] | Jasper M. Tomas[4] | Matthieu J. B. M. Pourquie[5]

[1]Whiffle Weather Finecasting Ltd, Molengraaffsingel 12, 2629 JD Delft, The Netherlands
[2]Delft University of Technology, Department of Geosciences & Remote Sensing, Stevinweg 1, 2628 CN Delft, The Netherlands
[3]Delft University of Technology, Department of Engineering Systems & Services, Jaffalaan 5, 2628 BX Delft, The Netherlands
[4]National Institute for Public Health and the Environment (RIVM), Antonie van Leeuwenhoeklaan 9, 3721 MA Bilthoven, The Netherlands
[5]Delft University of Technology, Faculty of Mechanical, Maritime and Materials Engineering (3mE), Mekelweg 2 2628 CD, Delft, The Netherlands

Correspondence
Stephan R. de Roode, Delft University of Technology, Department of Geosciences & Remote Sensing, Stevinweg 1, 2628 CN Delft, The Netherlands. Email: s.r.deroode@tudelft.nl

Marine stratocumulus clouds are frequently present over areas with rather low sea surface temperatures and in the presence of a warm thermal inversion layer. The phase changes of water, as well as the infrared cooling of air near the top of the cloud layer, are processes that cause positive buoyancy fluxes which tend to promote turbulence. The effect of low stratocumulus clouds on wind farm power is examined from a large-eddy simulation of the EUROpean Cloud Systems (EUROCS) model intercomparison case, which is based on observations of turbulence collected in marine stratocumulus during the First International Satellite Cloud Climatology Project Regional Experiment. A sensitivity experiment was performed in which the stratocumulus was excluded by setting the humidity to zero, while the same surface buoyancy flux was maintained. A comparison between the two simulation results shows that the turbulence that is produced in the stratocumulus cloud layer leads to a reduced wake effect and a subsequent enhancement of wind farm power most notably during nighttime. The control of stratocumulus on the wake is however hardly noticeable during daytime. This is due to the absorption of solar radiation that heats the cloud layer and which in turn tends to diminish turbulence. It is discussed that stratocumulus clouds are most likely to affect the wake structure during nighttime conditions if the boundary-layer depth is less than 500-700 m.

KEYWORDS:
Atmospheric boundary layers, stratocumulus clouds, large-eddy simulation, offshore wind farm power

## 1 | INTRODUCTION

Offshore production of wind energy is rapidly growing. Areas with a great potential for wind energy, such as the North Sea [1], are frequently affected by the presence of low stratocumulus clouds [2]. Stratocumulus is a very common cloud type, covering approximately 23% of the ocean surface in the annual mean [3]. However, the effect of low clouds on wind power has received hardly any attention in the literature. This is perhaps due to the perception that in general the presence of clouds does not matter for wind power. For example, Van Kuik and Peinke [4] state that "*traditionally, mesoscale models are evaluated on their ability to predict temperature, cloud cover, precipitation and other parameters of little relevance for wind power generation*". However, clouds have the ability to produce turbulence due to the temperature fluctuations that are caused by the condensation and evaporation of water, in addition to radiation effects [2,5]. In turn, boundary-layer turbulence is known to affect the wake structure behind wind turbines [6,7]. One may therefore ask whether clouds, or more particular those ones with their base heights in the lower few hundreds of meters, might affect the wind power?

Let us consider marine stratocumulus clouds which develop in the atmospheric boundary layer, often over relatively low sea surface temperatures. Figure 1 shows a schematic representation of the main features of stratocumulus clouds. The presence of a thermal inversion layer, which is defined as a sudden strong increase in the temperature across a vertical layer of just a few tens of meters, will trap the water vapor that is evaporated from the sea surface. The moistening of the boundary layer can lead to the saturation of air with water vapor and the subsequent formation of stratocumulus clouds at the top of the boundary layer. This is commonly observed in the subtropical branches of the Hadley cell, such as off the coasts of California and Peru, but also at more midlatitudinal regions like the North Sea in western Europe[2].

Stratocumulus clouds emit infrared radiation as a black body. If the sky above is clear, stratocumulus clouds will emit more infrared radiation than they absorb from the overlying atmosphere. The resulting loss of energy causes a strong cooling of the air near the top of the cloud layer. Because cooling keeps the saturation water vapor content low, this aids to the persistence of the cloud layer. It also results in the formation of organized cold downdrafts that keep the boundary layer vertically well mixed[8]. During daytime such a production of turbulent eddies will be reduced by solar heating of the cloud layer. The presence of turbulence in the stratocumulus-topped boundary layer raises the central question addressed in the present work: *does cloud-driven turbulence affect wind power?*

This study assesses wind farm power with and without the presence of stratocumulus clouds using a large-eddy simulation (LES) model that includes a wind turbine parameterization. This modelling approach was used because LES models have been demonstrated to capture the complex turbulence dynamics in stratocumulus rather well[9,10]. To capture a full diurnal cycle, including the effects of the solar heating of the cloud during daytime, the EUROpean Cloud Systems (EUROCS) stratocumulus model intercomparison case was selected for the simulations. This case is based on observations collected during two consecutive days as part of the First ISCCP (International Satellite Cloud Climatology Project) Regional Experiment (FIRE I)[9]. Another benefit of the modelling framework is that the effect of clouds on wind can be straightforwardly compared with clear sky conditions simply by changing the initial water vapor specific humidity well below its saturation value. This step effectively changes a stratocumulus topped boundary layer (STBL) to a clear convective boundary layer (CBL) weakly forced by a small surface buoyancy flux.

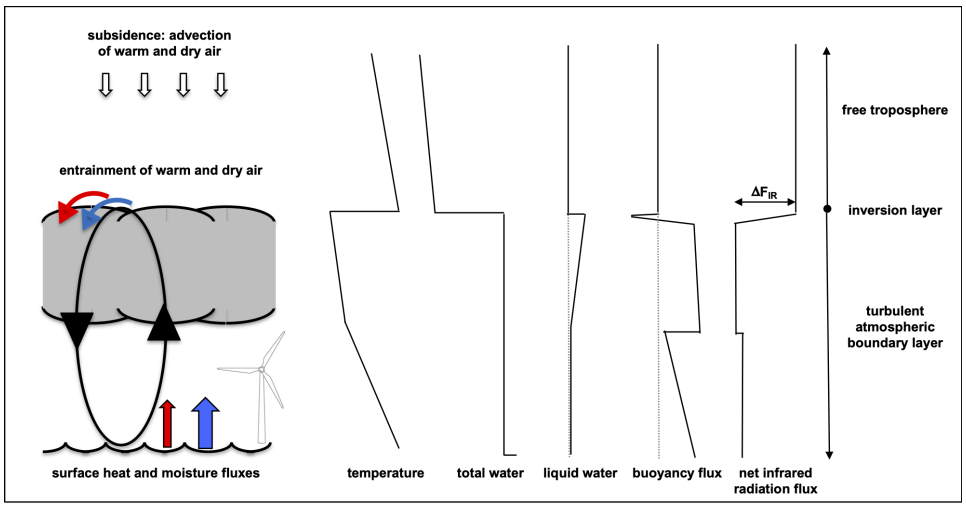


**FIGURE 1** Schematic representation of the mean vertical profiles of the temperature, total and liquid water, the buoyancy flux in the stratocumulus-topped boundary layer.

The set-up of the paper is as follows. The LES model and the set up of the cases are briefly summarized in Section 2. Section 3 reports the simulation results, with an emphasis on the wind speed, turbulence intensity and momentum fluxes, and the wake structure and power generation of a wind farm with and without the presence of stratocumulus. Finally it will be discussed under which conditions low clouds can be expected to have a notable effect on wind.

## 2 | MODEL DESCRIPTION AND EXPERIMENTAL SETUP

### 2.1 | Governing equations of the LES model

The LES model used in this study originates from the model described by Heus et al[11] and Schalkwijk et al[12] and is currently employed for both commercial and academic weather forecasting and simulation[13] by Whiffle Ltd. The general equations are summarized below.

Within the anelastic approximation, the continuity equation and the equation for momentum conservation are given by

$$\frac{\partial}{\partial x_j}\rho u_i = 0 \tag{1}$$

$$\rho\frac{\partial u_i}{\partial t} = -\frac{\partial \rho u_i u_j}{\partial x_j} + \frac{\partial \tau_{ij}}{\partial x_j} - \frac{\partial p'}{\partial x_j} + \delta_{i3}\rho B + \epsilon_{ij3} f (u_j - u_{\text{geo},j}) + \left(\frac{\partial \rho u}{\partial t}\right)_{\text{sources}}, \tag{2}$$

where $u_i$ ($i = 1, 2, 3$) are the resolved wind velocity components in the $x$, $y$ and $z$-direction, respectively, $\rho = \rho(z)$ is the base state density which is a function of $z$ only, $\tau_{ij}$ is the sub-grid stress tensor, $p'$ are the pressure fluctuations with respect to the mean, $B = -g\,(\rho'/\rho)$ is the buoyancy with $g$ the gravitational constant, $f$ is the Coriolis parameter and $u_{\text{geo}}$ is the geostrophic wind. The last term refers to a source term that may represent the forces due to wind turbines. Primes indicate deviations from the horizontal mean values.

The conservation equation for a scalar $\phi$ is given by

$$\rho\frac{\partial \phi}{\partial t} = -\frac{\partial \rho u_i \phi}{\partial x_j} - \frac{\partial F_{\phi,i}}{\partial x_j} + \left(\frac{\partial \phi}{\partial t}\right)_{\text{sources}} \tag{3}$$

where $\phi \in \{T_{hl}, q_t\}$ and

$$T_{hl} = T + \frac{1}{c_p}\left(gz - L_v q_l - L_s q_i\right) \tag{4}$$

$$q_t = q_v + q_l + q_i. \tag{5}$$

Here, $F_\phi$ is the sub-grid scalar flux, $T_{hl}$ the temperature based on the liquid/ice water static energy, $T$ is the temperature, $c_p$ is the specific heat of air at constant pressure, $L_v$ the heat of evaporation, $L_s$ the heat of sublimation and $q_t$ is the total (non-precipitating) specific humidity comprised of, respectively, the water vapor, cloud liquid water and cloud ice water specific humidity ($q_v$, $q_l$ and $q_i$).

The source term for $T_{hl}$ and $q_t$ contains a tendency due to large-scale advection. Further, $T_{hl}$ has an additional source term accounting for radiative heating/cooling.

For this study, the sub-grid stress tensor and sub-grid scalar fluxes are modelled using the Smagorinsky subgrid model[14].

### 2.2 | Wind turbine parameterization

In this study NREL 5 MW reference turbines are used, described in great detail by Jonkman et al[15]. The hub height was set to $90\,\text{m}$ in all cases. The wind turbines were modelled using an actuator disk parameterization, following the implementation of Meyers and Meneveau[16]. In this parameterization the total drag force on the flow is given by

$$F_{\text{tur}} = -\frac{1}{2}\rho A C_t' \overline{M_D}^2 \tag{6}$$

with $\rho$ the air density and $A = \pi R^2$ the frontal area of the rotor and $R$ the rotor radius. The disk-based thrust coefficient, $C_t'$, is obtained from the turbine design thrust curve by correcting for the resolved induction in the LES model. The rotor disk average wind speed $\overline{M_D}$ is computed for each wind turbine and filtered by a one-sided exponential time filter. The wind turbine force is distributed uniformly over the rotor disk and filtered with a Gaussian convolution kernel to ensure proper numerical behaviour[16,17].

The wind turbine power is given by

$$P = \frac{1}{2}\rho A C_p' \overline{M_D}^3, \tag{7}$$

with $C_p'$ the power coefficient, again corrected for resolved induction.

### 2.3 | Numerical setup

For the study of the structure of a single wake, a horizontal domain of $9.6\,\text{km} \times 4.8\,\text{km}$ at $50\,\text{m}$ resolution was selected. For simulation of a wind farm, the domain was enlarged to $12.8\,\text{km} \times 12.8\,\text{km}$. In both cases the vertical grid of the EUROCS is used ($1.2\,\text{km}$ domain height at $10\,\text{m}$ resolution).

Periodic boundary conditions are employed in the horizontal directions. At the edges of the domain the prognostic variables ($u$, $v$, $w$, $T_{hl}$, $q_t$) are relaxed at each time step towards the undisturbed values of an identical concurrent precursor simulation without wind turbines[18], to avoid recirculation of the wind turbine wakes.

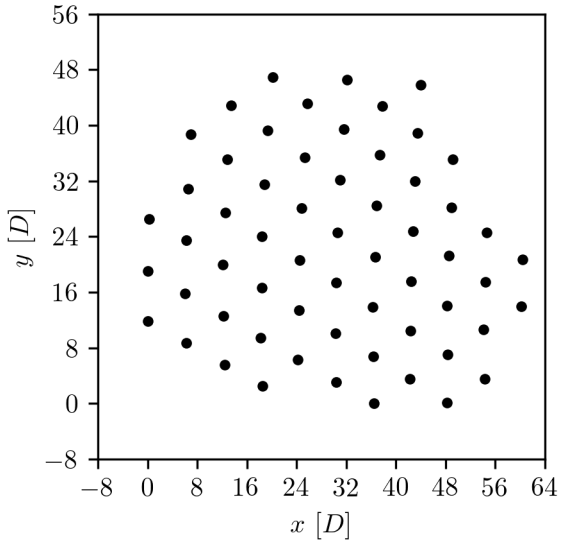


**FIGURE 2** Schematic representation of the wind farm layout used in this study. Axes are in units of rotor diameters $D$.

The selected wind farm layout is a version of the Prinses Amalia wind farm in the Dutch North Sea scaled up by a factor $126/80 = 1.575$, making it a realistic layout representative for a wind farm with wind turbines of $126\,\mathrm{m}$ diameter instead of the original $80\,\mathrm{m}$ diameter. See figure 2 for a schematic representation of the wind farm used in the simulations.

## 2.4 | Case description

The simulations in this work are based on the EUROpean Clouds Systems (EUROCS) stratocumulus model intercomparison case for LES and single-column model versions of operational weather forecast and climate models[9].

### 2.4.1 | The EUROCS stratocumulus case

The EUROCS stratocumulus case is widely used to study the dynamics of stratocumulus from high-resolution models and to improve parameterizations used in large-scale weather forecast and climate models[19,20]. This case is based on observations within and above the boundary layer off the coast of southern California on 14 and 15 July 1987[21]. The model simulations start at 14 July 08:00 UTC (00:00 local time) and last for 37 hours. The coordinates are $33^\circ$25'N and $119^\circ$30'W, with the Coriolis parameter $f = 8.0 \times 10^{-5}\,\mathrm{s}^{-1}$. For the present study the EUROCS case was selected because the turbulence in the boundary layer exhibits a distinct diurnal cycle due to the absorption of solar radiation by the cloud layer during daytime.

The EUROCS case is formulated in terms of the liquid water potential temperature $\theta_\mathrm{l}$, which can be readily converted to the temperature derived from the liquid/ice static energy, $T_{hl}$, used in the current LES model. The values of $\theta_\mathrm{l}$ and $q_\mathrm{t}$ in the boundary layer are constant as an initial condition, and give a cloud layer with its base and top at about 250 and 595 m, respectively, capped by a thermal inversion layer with jumps of the temperature and total specific humidity of 10 K and -3 $\mathrm{g\,kg}^{-1}$, respectively.

The magnitude of the geostrophic wind, $U_\mathrm{geo} = \sqrt{u_\mathrm{geo}^2 + v_\mathrm{geo}^2}$ is set to $6\,\mathrm{m\,s}^{-1}$. The angle of the geostrophic wind is chosen such that the hub-height wind speed is aligned with the positive $x$-direction.

The large-scale horizontal divergence of the horizontal wind $(U_\mathrm{ls}, V_\mathrm{ls})$ was prescribed at a constant value of $D = 1 \times 10^{-5}\,\mathrm{s}^{-1}$. Here we introduced the subscript 'ls' to indicate a large-scale field variable associated with the large-scale weather system in which the LES model domain is embedded. Conservation of mass dictates that a positive value for $D$ will drive a weak downward vertical velocity, which is usually referred to as large-scale subsidence ($W_\mathrm{ls}$). For constant $D$ the subsidence will vary linearly with height according to

$$D \equiv \left( \frac{\partial U_\mathrm{ls}}{\partial x} + \frac{\partial V_\mathrm{ls}}{\partial y} \right) = -\frac{\partial W_\mathrm{ls}}{\partial z}. \tag{8}$$

Although $W_\mathrm{ls}$ is small, usually of the order of $0.1\,\mathrm{cm\,s}^{-1}$ to $1\,\mathrm{cm\,s}^{-1}$, it has a non-trivial effect on the evolution of the boundary-layer depth in the sense that it acts to diminish the boundary-layer depth ($h$) thereby opposing its growth due to turbulent entrainment of air from just above the

inversion layer:

$$\frac{\partial h}{\partial t} = w_{\mathrm{e}} + W_{\mathrm{ls}}|_h, \tag{9}$$

with $w_{\mathrm{e}}$ the entrainment velocity[22]. The prescribed large-scale divergence rate approximately balances the diurnally averaged entrainment rate as simulated by the LES models that participated in the EUROCS model intercomparison case[9].

The surface fluxes of heat and moisture are computed from a prescribed constant sea surface temperature (SST) of $289\,\mathrm{K}$, which is about $1.5\,\mathrm{K}$ higher than the air temperature at the lowest model level. Furthermore, the Monin-Obukhov similarity relations used to compute the turbulent surface fluxes assume that the air just above the sea surface is saturated with water vapor. The surface roughness length is set to $2 \times 10^{-4}\,\mathrm{m}$. LES models that used this prescribed setup gave typical mean sensible and latent heat fluxes of 7 and $24\,\mathrm{W\,m^{-2}}$, respectively, during the last 24 hours of the simulation period. The heating and drying tendency of the free troposphere due to the large-scale subsidence is computed explicitly, whereas the tendencies of heat and moisture due to horizontal advection by the mean wind are prescribed. According to the case setup, the simulations applied the simplified yet accurate parameterizations for the infrared (long wave) and solar (short wave) radiation fluxes in the cloud layer[23,24]. The jump of the net infrared radiation flux near cloud top was set to $\Delta F_{\mathrm{IR}} = 70\,\mathrm{W\,m^{-2}}$.

#### 2.4.2 | Sensitivity experiment without stratocumulus: a clear convective boundary layer (CBL)

One of the main aims of the present study is to explore the role of turbulence in low stratocumulus clouds on wind farm power. To assess how the wake evolution would evolve without the presence of stratocumulus a sensitivity experiment with clear skies was performed. This was achieved simply by setting the initial total specific humidity to zero. Additionally, to ensure an identical surface forcing, the surface heat and moisture fluxes of the EUROCS case are prescribed at the surface. These steps result in a clear convective boundary layer, that is forced by a small positive surface buoyancy flux and a large-scale horizontal pressure gradient, with both conditions identical to the stratocumulus case. However, in order to maintain an approximate similar boundary layer depth as the stratocumulus case, the CBL case does neither apply large-scale subsidence nor horizontal advection of heat and moisture. In this way the free tropospheric state is not affected by horizontal or vertical advective tendencies thereby remaining in a steady state, similar to the stratocumulus case where subsidence warming of the free troposphere is compensated by a cooling tendency due to horizontal advection.

## 3 | LES RESULTS

Here we will present the LES results. In the remainder, the EUROCS case will be referred to as the stratocumulus-topped boundary layer (STBL). In section 3.1 we will first discuss the differences in the boundary layer structure of the STBL and CBL cases that were obtained from the LES without wind turbines. Next in section 3.2 we will analyse the impact of stratocumulus clouds on the wake structure and wind farm power. Day time is used to refer to the hour between 11:00 and 12:00 local time ($35\,\mathrm{h}$ to $36\,\mathrm{h}$ from the start of the simulation), and likewise nighttime is from 23:00 to 24:00 local time ($23\,\mathrm{h}$ to $24\,\mathrm{h}$ from the start of the simulation).

### 3.1 | Boundary layer evolution, wind speed and turbulence

Figure 3 shows the temporal evolution of the boundary layer height $h$ and the entrainment velocity $w_{\mathrm{e}}$ for the STBL and CBL cases, as well as the stratocumulus cloud base height $z_{\mathrm{b}}$ and cloud top height $z_{\mathrm{t}}$.

The stratocumulus boundary layer height exhibits only a weak diurnal variation and remains rather close to its initial height of about $600\,\mathrm{m}$. In accord with the aim of the particular setup of the CBL case its height remains rather close the STBL height during the simulation period. The stratocumulus cloud base height displays a rising during daytime as a result of the warming and subsequent evaporation of the cloud liquid water, while the cloud tends to get thicker (decreasing cloud base height) during the night.

The entrainment rate in the clear convective boundary layer is proportional to the surface buoyancy flux, and tends to become smaller for larger values of the temperature jump across the inversion layer. As evident from the LES results, entrainment is higher in stratocumulus than in a CBL, a finding that is common for those two boundary-layer regimes[25]. The large entrainment rates in stratocumulus clouds are due to the production of turbulence in the cloud layer, with as causes most notably latent heating associated with phase changes of water and the strong infrared radiative forcing that takes place near cloud top. The infrared radiative forcing is often observed to be much larger than the surface sensible heat fluxes that drive the turbulence in the marine boundary layer. For example, in the present study the sensible heat flux is of the order of $10\,\mathrm{W\,m^{-2}}$ whereas the longwave radiative forcing at cloud top is $70\,\mathrm{W\,m^{-2}}$. The heating of the cloud layer by absorption of solar radiation however acts to decrease cloud-top entrainment as shown in Fig. 3.

Figure 4 compares the temporal evolution of the wind speed $U$ and resolved turbulence kinetic energy (TKE) for the CBL and STBL cases averaged over the horizontal domain and vertical rotor extent ($27\,\mathrm{m}$ to $153\,\mathrm{m}$) and Figure 5 shows the hourly-mean vertical profiles during daytime

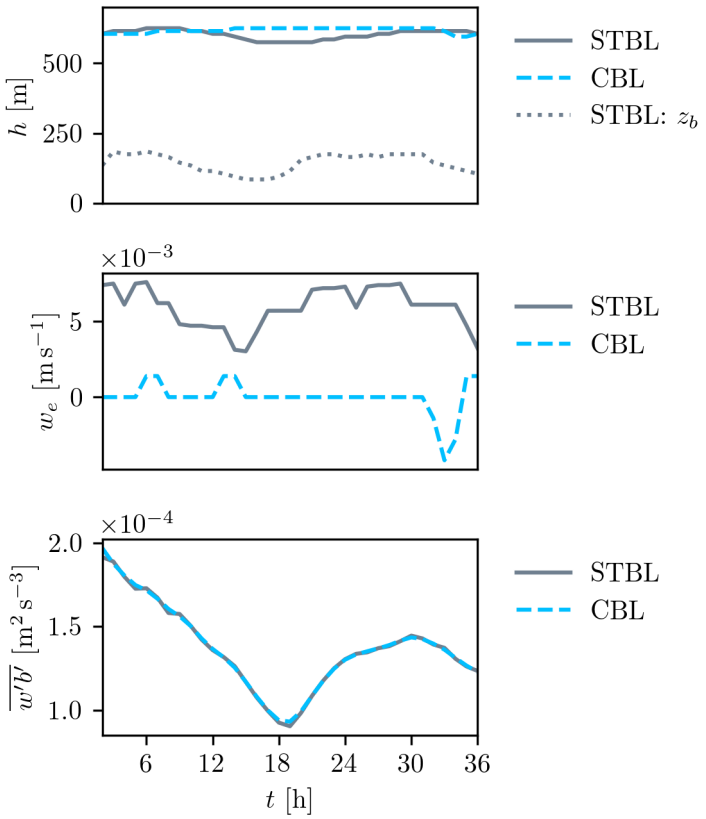


**FIGURE 3** Time evolution of the boundary layer height $h$ and cloud base height $z_b$ (top figure), entrainment velocity (middle) and surface buoyancy flux (bottom) for the STBL and CBL cases.

and nighttime. The wind speed in the lower part of the STBL is rather constant in time and is somewhat lower compared to the CBL case. An inspection of the vertical profile of $\overline{u'w'}$ during daytime shows a small change in its vertical gradient near cloud base indicating different magnitudes of the fluid friction in the subcloud and cloud layers.

The distinct diurnal cycle in the TKE in the STBL, with rather large values during nighttime, can be understood from the in-cloud buoyancy production of TKE. Figure 6 shows that during nighttime in both the LES results and observations the in-cloud buoyancy fluxes and the TKE are much larger in the STBL than in the CBL cases. The large jump in the buoyancy flux near the top of the boundary layer is a distinct feature of stratocumulus cloud decks. The strong infrared radiative loss near the top of the cloud layer causes a direct local cooling of the air. This results in the formation of cold downdrafts, which, in turn, produces positive buoyancy fluxes in the cloud layer. In addition, the condensation (evaporation) of water vapor in updrafts (downdrafts) promotes a positive buoyancy flux, too. Hence both phase changes of water and infrared cooling of the cloud top are the key processes that can generate rather strong turbulence throughout the cloud-topped boundary layer, as is evident from the large TKE values present during nighttime. However, during daytime the infrared cooling is partly counteracted by a heating of the cloud layer by the absorption of solar radiation. This warming effect may stabilize the cloud layer with respect to its sub-cloud layer below. This kind of stratification is called decoupling [26,27]. In general, the heating of the cloud layer by solar radiation causes a reduction of turbulence during daytime conditions. Last we note that the CBL and STBL both exhibit a negative value for the buoyancy flux at the top of the boundary layer, which is due to entrainment and the subsequent downward mixing of relatively warm air from just above the inversion layer.

## 3.2 | Wake structure behind a single turbine

A comparison for the wake evolution behind a single turbine is shown in Fig. 7. The wind velocity deficit (VD) as shown in this figure is defined as

$$\mathrm{VD} = \frac{U_{\mathrm{precursor}} - U_{\mathrm{cursor}}}{U_{\mathrm{precursor}}}, \tag{10}$$

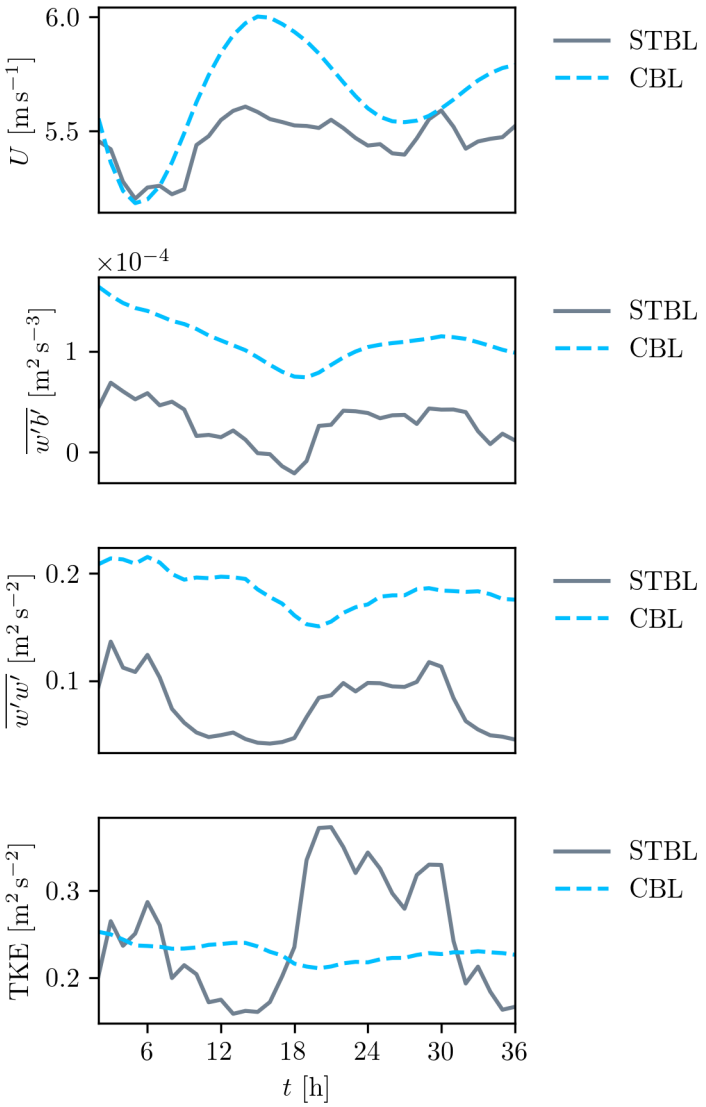


**FIGURE 4** Development of horizontal wind speed (top) and the turbulence kinetic energy per unit mass (TKE) (bottom) for the STBL and CBL cases. Values are averaged over the horizontal domain and the vertical extent of the rotor.

where the subscript 'precursor' indicates wind speed values from the concurrent precursor simulation without wind turbine that is driving the cursor with wind turbines. The enhanced turbulence that is present in the nighttime STBL strongly reduces the wake length. This impact of turbulence on the wake structure is qualitatively similar to what has been found for other atmospheric boundary-layer regimes. For example, stronger wake effects have been reported under conditions of low turbulence intensities such as observed in stably stratified boundary layers [28,7,29,30]. However, the weakening of turbulence in the STBL during the day, which results from the solar heating of the cloud layer, causes a wake structure similar to what is found for the CBL case.

## 3.3 | Wind farm power

For wind farms, the angle with which the wind approaches the wind farm plays a substantial role in how much wake effects play a role on the power output of the farm. A maximum wake effect can be expected if the wind direction is perfectly aligned with the turbine rows downstream. The wind direction, however, changes during the simulation. For the results below, the initial wind direction and the direction of the pressure forcing for each case was chosen such that the average wind direction from $12\,\mathrm{h}$ to $36\,\mathrm{h}$ from the start of the simulation is from the west ($\phi = 270°$).

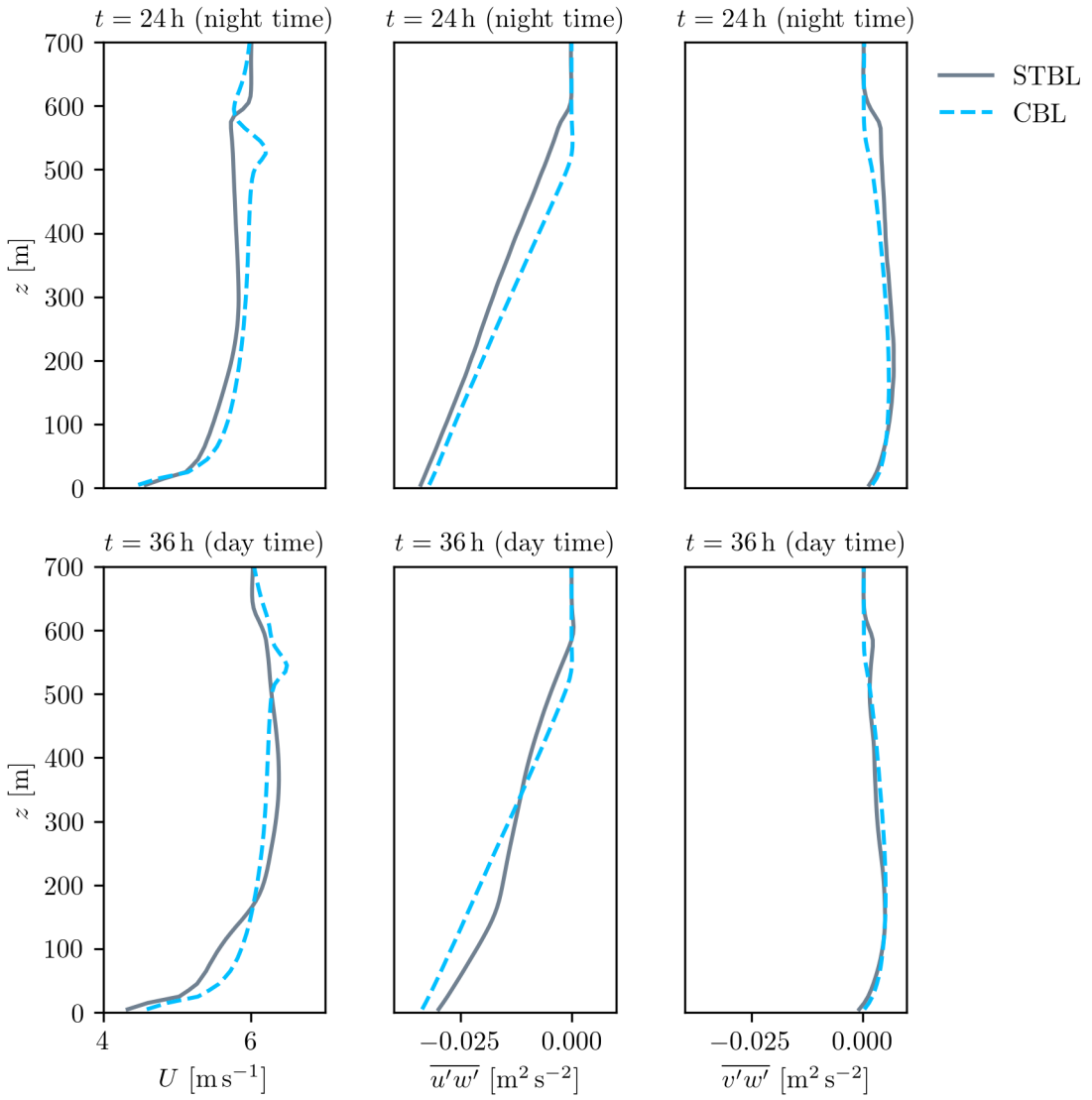


**FIGURE 5** Vertical profile of wind speed (left) and vertical momentum fluxes (middle and right) at night time (top) and day time (bottom) averaged in time over the preceding hour.

Figure 9 shows the wind velocity deficit at hub height at day time and night time. The higher turbulence levels in the night time STBL are evident from the overall shorter wake extent and the larger variation in wind turbine yaw angles due to local wind direction fluctuations.

The three main controls on wind farm power productions are wind speed, turbulence and wind direction in relation to wind farm layout. Figure 8 shows the wind direction of the STBL and CBL cases is similar during the simulation period. Also, the present wind farm layout was selected for not having an obvious row-column structure to further limit the sensitivity to wind direction. This leaves the impact of wind speed and turbulence.

To consider wind speed and turbulence together, we examine the accumulated power output of the wind farm as function of time in the different cases, see Figure 10. During the day the CBL case shows higher power production, whereas during the night the production in the STBL is substantially higher. However, this might not be surprising as figure 4 shows a clearly higher wind speed in the CBL case during the day and lower wind speed during the night when compared to the STBL. Also interesting to note are the stronger hour-to-hour variations in the STBL, showing the impact of the stratocumulus cloud deck also on the larger scale dynamics of the atmosphere.

To eliminate the effect of wind speed, we define a wind farm efficiency

$$\eta = \frac{P}{\frac{1}{2}\rho A U^3 N_{\mathrm{T}}}, \tag{11}$$

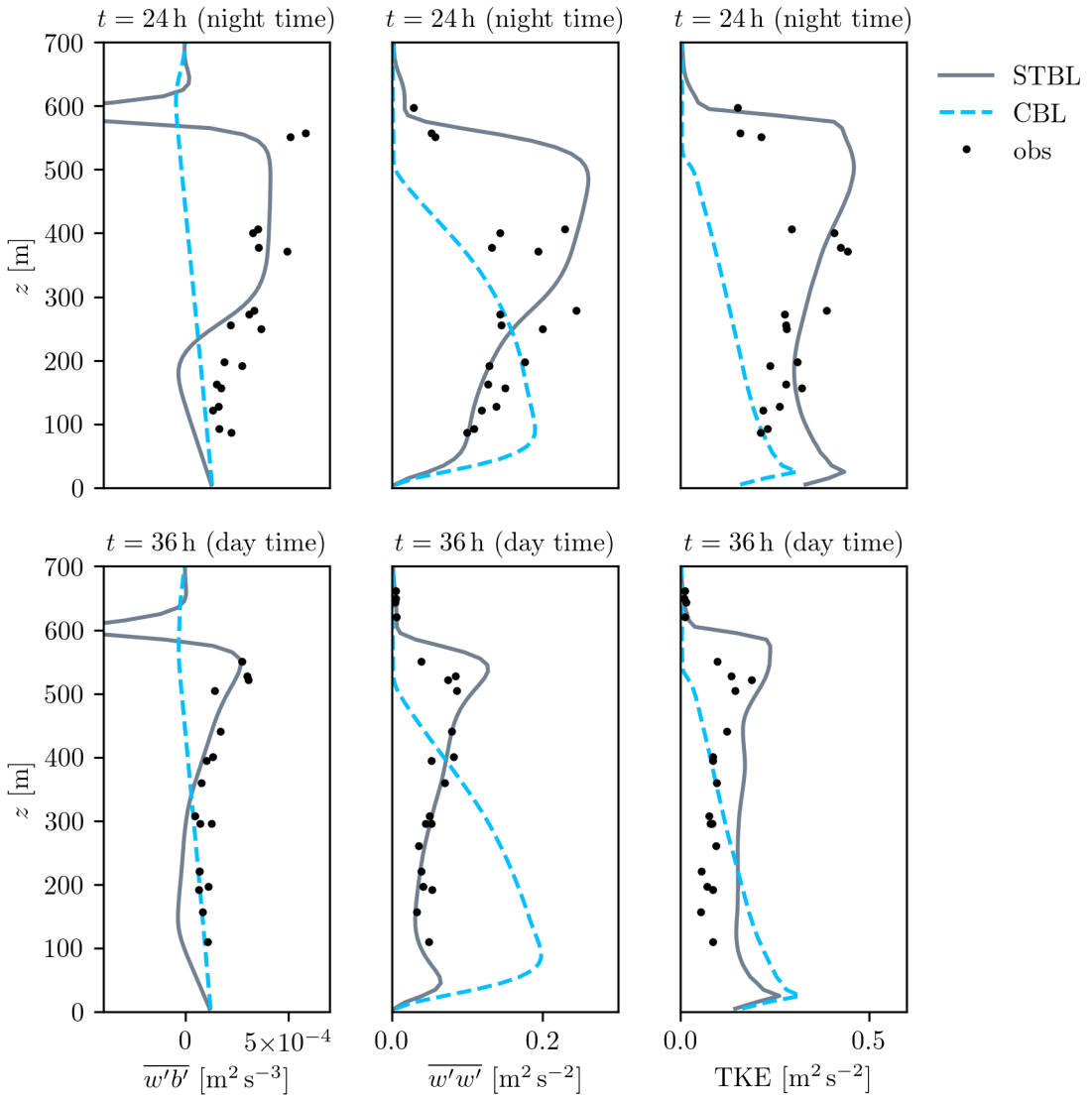


**FIGURE 6** Vertical profiles of the hourly-mean total buoyancy flux (left), resolved vertical velocity variance (middle) and resolved turbulence kinetic energy (right) in the STBL and CBL during day time (top) and night time (bottom). The observations corresponding to the STBL case are taken from Duynkerke et al[9].

with $N_\mathrm{T}$ the number of wind turbines in the farm. The aim of this efficiency factor, is to identify the role of wake effects on the total wind farm power.

The bottom plot in Figure 10 shows that the efficiency of the wind farm in the CBL case is nearly constant with time. The higher power production during the night can therefore be fully attributed to the higher wind speed. In contrast, the efficiency of the wind farm during stratocumulus conditions shows a distinct diurnal cycle, being around $20\,\%$ higher during the night. The pattern in $\eta$ shows a clear correspondence with the diurnal cycle of TKE (Figure 4), confirming that the increase of wind farm efficiency can be attributed to a more efficient turbulent mixing dissolving the wakes in the farm.

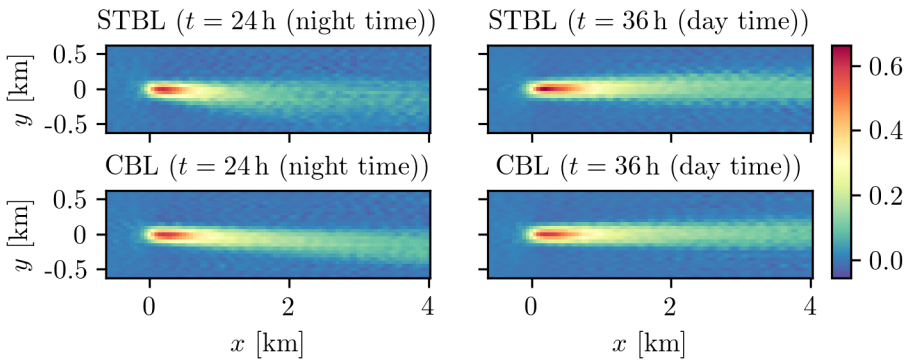


**FIGURE 7** The hourly average hub height velocity deficit in the STBL (top) and CBL (bottom) for day time (left) and night time (right).

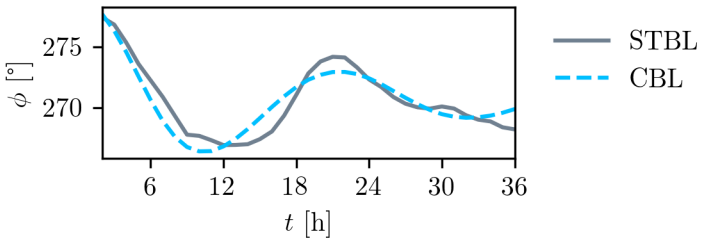


**FIGURE 8** The hub height wind direction $\phi$ for the STBL and CBL cases.

## 4 | DISCUSSION

We have found that under similar wind conditions, in terms of its speed and direction, wind farm power will be enhanced if the wake effect is reduced by the turbulence that is produced in the stratocumulus cloud deck. However, the simulation results also indicate that stratocumulus control on the wake depends on the time of the day, with a notable effect found only during the night. This leads to the question under which conditions stratocumulus clouds are expected to modify wind farm power. This will now be discussed on the basis of observational findings, studies based on LES results as well as theory.

### 4.1 | Conditions that favour a rapid wake recovery

Turbulence in stratocumulus is produced by infrared cooling of the air near cloud top as well as phase changes of water. Radiatively cooled air will drive negatively buoyant turbulent downdrafts, which cause positive in-cloud buoyancy fluxes that, in turn, produce vertical velocity variance. Likewise, if surface-driven convective plumes become saturated with water vapor, the latent heat release due to condensation of water will promote positive buoyancy fluxes in the cloud layer. If the updrafts can rise from the ground surface to the top of cloud, and vice versa for downdrafts, they will stir the boundary layer to a vertically well mixed state, a situation that is usually found if the stratocumulus-topped boundary layer height is below 500-700 m [31]. In this case the vertical velocity variance profile will have a single maximum value near the middle of the boundary layer. In turn, the presence of strong vertical velocity fluctuations will promote the exchange of horizontal momentum across the wake interface.

By contrast, if the cloud layer is warm with respect to the subcloud layer underneath, which may result from its absorption of solar radiation, even the latent heat release may not be sufficient to let the surface-driven rising plumes become positively buoyant with respect to their environment, as is found in the present LES results. As opposed to a vertically well-mixed state, this situation is called decoupling [2]. This may develop also as a result of a strong cloud-top entrainment of warm and dry air from just above the inversion layer [26]. In this case it will be more difficult for cloudy downdrafts to maintain a negative buoyancy that drives their downwards acceleration. Decoupling is frequently observed during daytime when the cloud layer is heated by the sun. In addition, stratocumulus-topped boundary layers that have reached heights above 500-700 m, for example as a result of a strong entrainment velocity at cloud top, often appear to be decoupled [31]. Given the fact that stratocumulus cloud layers are usually

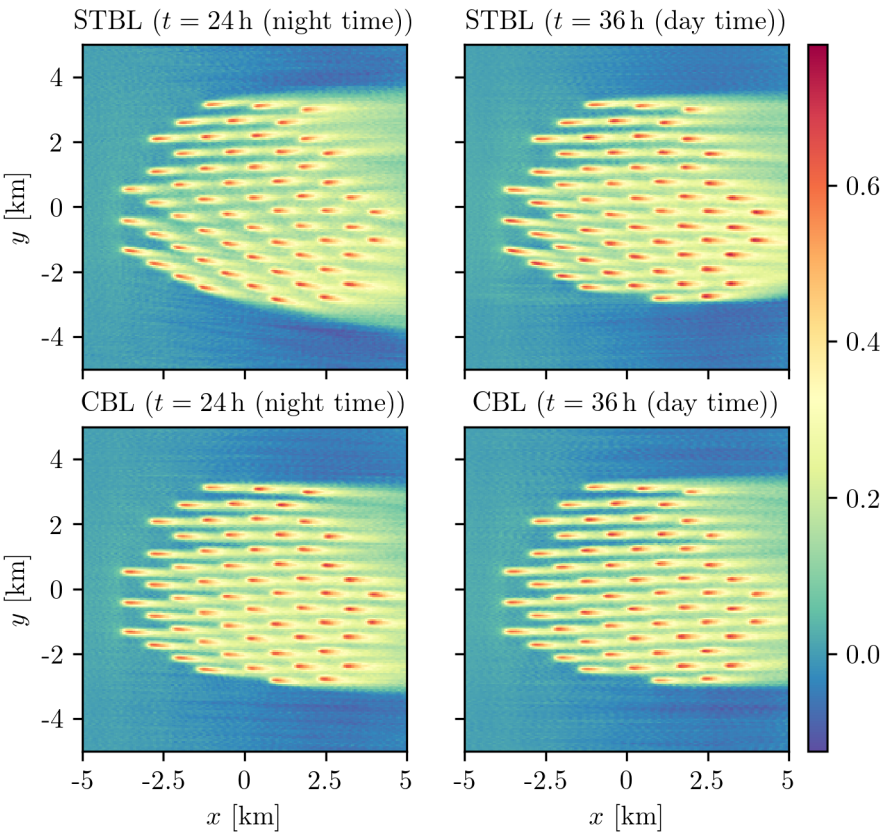


**FIGURE 9** The hub height velocity deficit for the STBL (top) and CBL (bottom) cases for night time (left) and day time (right).

observed to be only a few hundreds of meters thick, the stratocumulus cloud base height in deep decoupled boundary layers will be located at heights well above the wind turbines.

## 5 | CONCLUSIONS

This study discusses the impact of low clouds on wind farm power by means of a large-eddy simulation (LES) of the diurnal cycle of an observed stratocumulus cloud layer. To identify the contribution of cloud-driven turbulence on the evolution of the wake another sensitivity experiment was performed without moisture. This change resulted in a clear convective boundary layer that was only weakly forced by a small positive buoyancy flux at the sea surface.

An enhancement of turbulence produced in the cloud layer causes a reduction of the wake effect, most notably during the night. During daytime the absorption of solar radiation and the subsequent heating of the cloud layer stabilizes the boundary-layer resulting in weaker turbulence, leaving hardly any impact on wind farm power as compared to the cloud-free case. A noticeable effect of low clouds on wind farm power can be expected if the cloud base is near the turbine as this will likely facilitate cloud-induced turbulence to reach the wake area. Observations and theory suggest that enhanced turbulence in the lower few hundreds of meters of the atmosphere can be expected if the cloud-top height is below 500 up to about 700 m.

The conclusions drawn in the present work are based on a single case study. However, the physical processes like phase changes of water and infrared cooling of air near the cloud top are always at play in stratocumulus decks and are well known to enhance turbulence. Because low marine clouds are frequently present over areas with wind farms, such as the North Sea, a more detailed assessment of their impacts on wind farm power, but also on the turbulence structure, including wind gusts, is recommended. Future work could therefore focus on a systematic study of cloud-induced turbulence in the widest possible range of real-weather conditions to assess the quantative impact of low clouds on the energy yield of offshore wind farms in areas sensitive to the formation of low clouds.

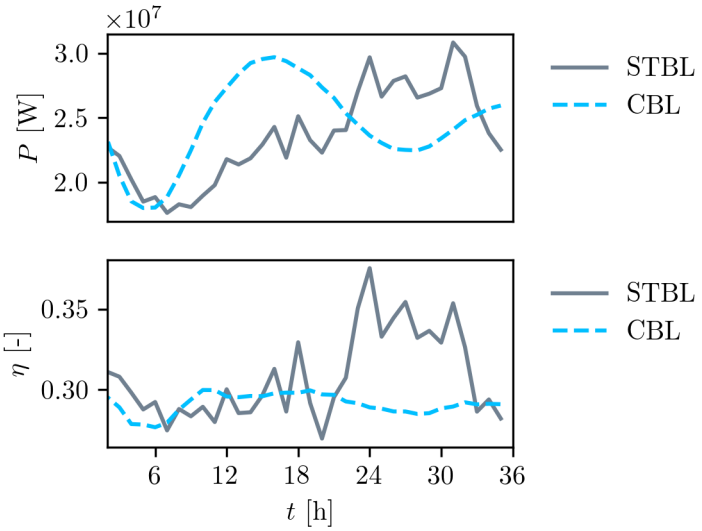


**FIGURE 10** Development of total power generated by the wind farm (top) and wind farm efficiency (bottom).

## ACKNOWLEDGMENTS

The research leading to these results has received funding from the Netherlands Organization for Scientific Research (NWO), Toegepaste en Technische Wetenschappen (TTW), under grant agreement 18657.

## References

1. Kalverla PC, Holtslag AA, Ronda RJ, Steeneveld GJ. Quality of wind characteristics in recent wind atlases over the North Sea. *Quart. J. Roy. Meteorol. Soc.* 2020; 146(728): 1498–1515.

2. Nicholls S. The dynamics of stratocumulus: aircraft observations and comparisons with a mixed layer model. *Quart. J. Roy. Meteorol. Soc.* 1984; 110: 783–820.

3. Wood R. Stratocumulus clouds. *Mon. Weather Rev.* 2012; 140: 2373–2423.

4. Van Kuik G, Peinke J. *Long-term research challenges in wind energy-a research agenda by the European Academy of Wind Energy*. 6. Springer . 2016.

5. Nicholls S. The structure of radiatively driven convection in stratocumulus. *Quart. J. Roy. Meteorol. Soc.* 1989; 115: 487–511.

6. Mirocha J, Kosovic B, Aitken M, Lundquist J. Implementation of a generalized actuator disk wind turbine model into the weather research and forecasting model for large-eddy simulation applications. *Journal of Renewable and Sustainable Energy* 2014; 6(1): 013104.

7. Aitken ML, Kosović B, Mirocha JD, Lundquist JK. Large eddy simulation of wind turbine wake dynamics in the stable boundary layer using the Weather Research and Forecasting Model. *Journal of Renewable and Sustainable Energy* 2014; 6(3): 033137.

8. Turton JD, Nicholls S. A study of the diurnal variation of stratocumulus using a multiple mixed layer model. *Quart. J. Roy. Meteorol. Soc.* 1987; 113: 969–1009.

9. Duynkerke PG, Roode dSR, Zanten vMC, et al. Observations and numerical simulations of the diurnal cycle of the EUROCS stratocumulus case. *Quart. J. Roy. Meteorol. Soc.* 2004; 130: 3269–3296.

10. Van der Dussen JJ, J. J, Roode dSR, et al. The GASS/EUCLIPSE model intercomparison of the stratocumulus transition as observed during ASTEX: LES results. *J. Adv. Model. Earth Syst.* 2013; 5: 1–17.

11. Heus T, van Heerwaarden CC, Jonker HJJ, et al. Formulation of the Dutch Atmospheric Large-Eddy Simulation (DALES) and overview of its applications. *Geosci. Model Development* 2010; 3: 415–444. doi: 10.5194/gmd-3-415-2010

12. Schalkwijk J, Jonker HJ, Siebesma AP, Van Meijgaard E. Weather forecasting using GPU-based large-eddy simulations. *Bulletin of the American Meteorological Society* 2015; 96(5): 715–723.

13. Gilbert C, Messner JW, Pinson P, et al. Statistical post-processing of turbulence-resolving weather forecasts for offshore wind power forecasting. *Wind Energy* 2020; 23(4): 884–897.

14. Smagorinsky J. General circulation experiments with the primitive equations: I. The basic experiment. *Monthly weather review* 1963; 91(3): 99–164.

15. Jonkman J, Butterfield S, Musial W, Scott G. Definition of a 5-MW reference wind turbine for offshore system development. tech. rep., National Renewable Energy Lab.(NREL), Golden, CO (United States); 2009.

16. Meyers J, Meneveau C. Large eddy simulations of large wind-turbine arrays in the atmospheric boundary layer. In: ; 2010: 827.

17. Calaf M, Parlange MB, Meneveau C. Large eddy simulation study of scalar transport in fully developed wind-turbine array boundary layers. *Physics of Fluids* 2011; 23(12): 126603.

18. Stevens RJ, Graham J, Meneveau C. A concurrent precursor inflow method for large eddy simulations and applications to finite length wind farms. *Renewable energy* 2014; 68: 46–50.

19. Ackerman AS, Kirkpatrick MP, Stevens DE, Toon OB. The impact of humidity above stratiform clouds on indirect aerosol forcing. *Nature* 2004; 432: 1014–1017. doi: 10.1038/nature01174

20. Hourdin F, Jam A, Rio C, et al. Unified parameterization of convective boundary layer transport and clouds with the thermal plume model. *Journal of Advances in Modeling Earth Systems* 2019; 11(9): 2910–2933.

21. Hignett P. Observations of the diurnal variation in a cloud-capped marine boundary layer. *J. Atmos. Sci.* 1991; 48: 1474–1482.

22. Stevens B. Bulk boundary-layer concepts for simplified models of tropical dynamics. *Theor. Comput. Fluid. Dyn.* 2006. doi: DOI 10.1007/s00162-006-0032-z

23. Larson VE, Kotenberg KE, Wood NB. An analytic longwave radiation formula for liquid layer clouds. *Mon. Weather Rev.* 2007; 135: 689–699.

24. Joseph JH, Wiscombe WJ, Weinman JA. The delta-Eddington approximation for radiative flux transfer. *J. Atmos. Sci.* 1976; 33: 2452–2459.

25. Stevens B. Entrainment in stratocumulus-topped mixed layers. *Quart. J. Roy. Meteorol. Soc.* 2002; 128: 2663–2690.

26. Bretherton CS, Wyant MC. Moisture transport, lower-tropospheric stability, and decoupling of cloud-topped boundary layers. *J. Atmos. Sci.* 1997; 54: 148–167.

27. De Roode SR, Sandu I, Dussen v. dJJ, et al. Large eddy simulations of EUCLIPSE/GASS Lagrangian stratocumulus to cumulus transitions: Mean state, turbulence, and decoupling. *J. Atmos. Sci.* 2016; 73: 2485-2508.

28. Magnusson M, Smedman AS. Influence of atmospheric stability on wind turbine wakes. *Wind Engineering* 1994: 139–152.

29. Abkar M, Porté-Agel F. Influence of atmospheric stability on wind-turbine wakes: A large-eddy simulation study. *Physics of fluids* 2015; 27(3): 035104.

30. Dörenkämper M, Witha B, Steinfeld G, Heinemann D, Kühn M. The impact of stable atmospheric boundary layers on wind-turbine wakes within offshore wind farms. *Journal of Wind Engineering and Industrial Aerodynamics* 2015; 144: 146–153.

31. Wood R, Bretherton CS. Boundary layer depth, entrainment, and decoupling in the cloud-capped subtropical and tropical marine boundary layer. *J. Climate* 2004; 17: 3576–3588.